applied sciences

MDPI

Article

Development of a Structural Monitoring System for Cable Bridges by Using Seismic Accelerometers

Seong-Hoon Jeong [1,*], Won-Seok Jang [1], Jin-Won Nam [2], Hohyun An [3] and Dae-Jin Kim [4]

[1] Department of Architectural Engineering, Inha University, Incheon 22212, Korea; jang@inha.ac.kr
[2] Atech Solution, Inc., Uiwang 16006, Korea; jwnam72@gmail.com
[3] TM EnC, Inc., Seongnam 13209, Korea; truelies9601@gmail.com
[4] Department of Architectural Engineering, Kyung Hee University, Yongin 17104, Korea; djkim@khu.ac.kr
* Correspondence: jeong@inha.ac.kr; Tel.: +82-32-860-7585

Received: 19 December 2019; Accepted: 15 January 2020; Published: 20 January 2020

check for updates

Abstract: In this study, a structural health monitoring system for cable-stayed bridges is developed. In the system, condition assessment of the structure is performed based on measured records from seismic accelerometers. Response indices are defined to monitor structural safety and serviceability and derived from the measured acceleration data. The derivation process of the indices is structured to follow the transformation from the raw data to the final outcome. The process includes, noise filtering, baseline correction, numerical integration, and calculation of relative differences. The system is packed as a condition assessment program, which consists of four major process of the structural health evaluation: (i) format conversion of the raw data, (ii) noise filtering, (iii) generation of response indices, and (iv) condition evaluation. An example set of limit states is presented to evaluate the structural condition of the test-bed cable-stayed bridge.

Keywords: structural health monitoring; cable-stayed bridge; seismic accelerometer; response indices

1. Introduction

For the public safety management, the use of a structural health evaluation system based on seismic accelerometers is in increasing demand. Due to the recent development of sensor and measurement technologies, the number of monitoring systems installed on important structures such as cable bridges is rapidly increasing [1–3]. The range of the application of the structural health monitoring is very wide. Various researches have been performed to examine the condition of the infrastructure for durability issues [4–6]. Besides the issues of the condition assessment, structural health monitoring systems can be deployed to ensure that the built structure satisfies the design requirements and assumptions [7]. For example, the effect of spatial variation of seismic ground motions on the super structures of long-span bridges has been studied using the measured data during the earthquake [8]. Investigation of damping mechanisms and estimation of damping values based on the real structure behavior are performed [9]. Researches on damage detection of bridge structures have been continuously developed on the basis of the sensor and communication technologies. Structural health monitoring technologies based on imaging and vision sensors [10,11], and microelectromechanical systems (MEMS) sensors [12,13] can be considered as emerging technologies [14]. Application of wireless sensor network [15,16] for the condition assessment has evolved to internet of things (IOT) [17,18] based structural health monitoring system.

While the state-of-the-art research and novel sensors lead the progress of technologies in structural health monitoring of bridges, it should be noted that detailed information on the analysis and interpretation of data is essential for engineers to construct the monitoring system. The originality of this study lies in providing details of monitoring algorithms for interpretation of the measured data in the post-earthquake condition assessment based on seismic accelerometers. This study focuses on practical information to deal with the issues encountered in data processing procedures and calculation of response indices, which have not been treated enough in the previous studies.

The condition assessment system is useful for pre-earthquake disaster planning and post-earthquake recovery programs [19]. The majority of the monitoring software in the field are developed by the equipment providers and hence have not been verified their reliability in structural condition assessment. Therefore, it is of importance to develop reliable health monitoring software that can generate appropriate response indices of the structure [20–22]. In this paper, major components of a health monitoring software and a data matrix to generate response indices are discussed. The data matrix represents the interrelationship between the measured data from the seismic accelerometers and the response indices.

2. Structure of the Monitoring System

The system is composed of four parts each of which corresponds to the major process of the structural health evaluation (Figure 1). The first part is the format conversion process where the compressed format of the acquired acceleration data is converted to text format for numerical calculations (Figure 2). The Standard for the Exchange of Earthquake Data (SEED) and its subset with reduced metadata (miniSEED) are widely used for recording the raw data from seismic accelerometers. These formats are maintained by the international Federation of Digital Seismograph Networks (FDSN) and additional details can be found elsewhere [23]. Since the SEED and the miniSEED are data formats devised mainly for the archival and exchange of seismological time series, format conversions are needed for processing of data. The compressed format of the raw data needs to be converted to text data for further analysis procedures. Physical factors are needed to make text data from the raw data, which is the record of changes in voltage acquired from the accelerometer sensors. The physical factor is calculated from the sensitivity value for the recorder and the response value for the accelerometer. The physical factor is calculated from the sensitivity value for the recorder and the response value for the accelerometer and acceleration in gal is obtained by multiplying the physical factor to the count values in the raw data, where, gal is defined as 1 cm per second squared (1 cm/s^2). For instance, the physical factor is calculated as 2.336×10^{-4} from Equation (1), if the sensitivity and the response values are given as 1.1921 μV/count and 0.5102 V/(m/s^2), respectively.

$$\text{Physical Factor} = \frac{1.1921}{0.5102} \cdot \frac{\frac{\mu\text{V}}{\text{count}}}{\frac{\text{V}}{\frac{\text{m}}{\text{sec}^2}}} = 2.336 \times 10^{-4} \text{gal/count}. \quad (1)$$

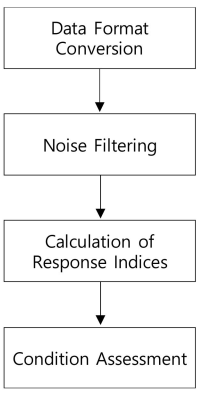

Figure 1. Major processes of the monitoring system.

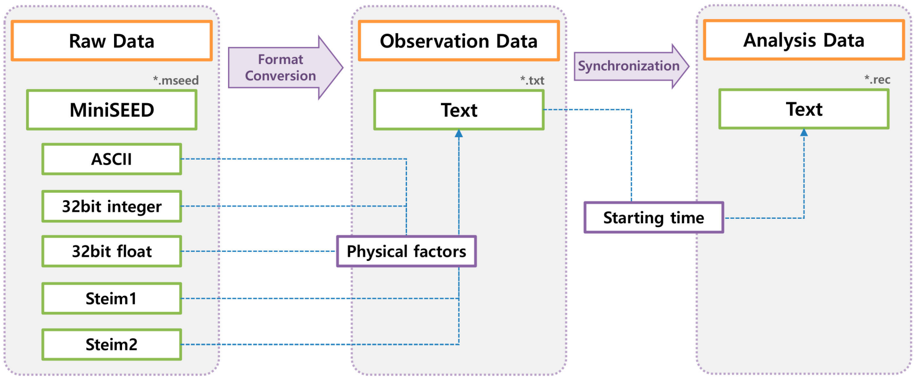

Figure 2. Conversion process from miniSEED to ASCII data formats.

The second step is the noise filtering process. Since there are various sources of noise in the measured accelerogram, processing data without noise filtering will mislead the analysis result, as shown in Figure 3. Details on the noise filtering schemes for seismic accelerometers are given elsewhere [24]. Raw data of acceleration records include noise from various sources such as instrument's installation conditions and environments. In general, low-frequency noise below 0.1 Hz is called microseism, and high-frequency noise above 0.5 Hz is called microtremor [25,26]. Noises are continuously generated, change in time and space and vary across all frequency ranges [27]. It has been shown that the applications of the noise filtering process and the base-line correction have a significant effect on displacement time histories derived through double integration of acceleration time histories [28]. If noise is not filtered from the raw data, the noises are accumulated to be diverged results. Butterworth filter is generally preferred since the shape of the curve is relatively sharp at the corner period and there is no riffle in the band range, as shown in Figure 3.

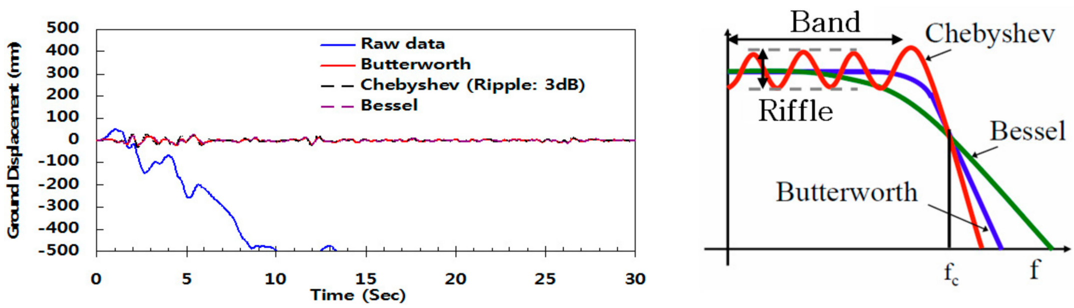

Figure 3. Displacement response histories with/without filters and comparison of noise filters.

The third step is the calculation of the response indices, which are used for condition assessments. In this study, response indices are categorized as time and frequency domain indices based on the calculation process. While response histories of the time domain indices are obtained from time-integration on the accelerograms, frequency domain indices are obtained from Fourier transformation. Displacements at measurement points are obtained through double-integration of acceleration time histories at the corresponding locations and relative displacements are derived by subtracting the displacement at one location from the displacement at the other location. For instance, the relative displacement of the pylon is calculated by subtracting the displacement at the bottom of the pylon from the displacement at the top of the pylon.

The interrelationship between the measured data of a cable-stayed bridge and analysis results, which is used for the response indices are represented in Figure 4. As shown in the latter figure, a whole set of data in this system is organized in the form of 2D matrix. This form of data set is devised to pursue efficiencies in database accommodation and expandability to other structures.

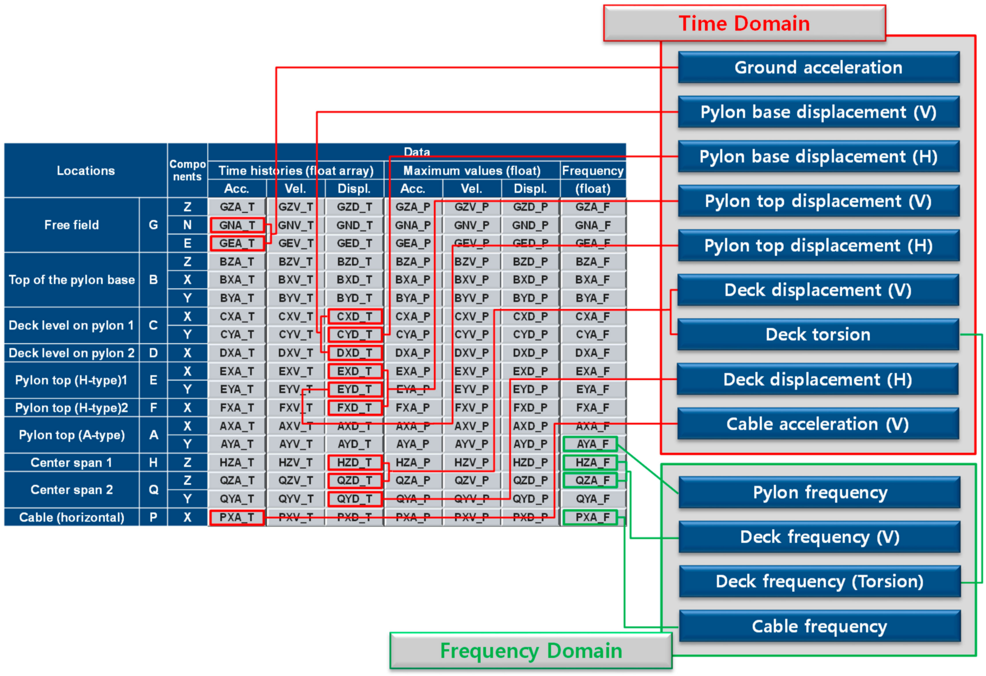

Figure 4. Overview of the data processing procedures and response indices.

While damage indicating methods have been traditionally developed based on relative displacements of the structure [29], studies on relationship between the degree of structural deterioration and the changes in natural frequencies have shown that the pattern of changes in natural frequencies is affected by the location and the degree of damage. The change of natural frequencies can be used as a damage indicator since it is sensitive to the stiffness change of a structure [30]. In the study performed by the National Disaster Management Institute [20], a method to identify the structural damages based on the change in the natural frequencies is presented. Earlier studies on the measurement of dynamic responses showed that the detection of a structural damage is feasible by observing changes in natural frequencies due to damages on the structural members [30,31]. Based on the recent development on sensor and measurement technologies, advanced studies on the relationships on vibration modes and structural damages have been performed to identify the location of damages and show that a stiffness decrease due to a structural deterioration causes the change of natural frequencies in lower modes [32–36].

The fourth step is the condition evaluation of the bridge structure. The latter process, in general, includes decision of limit states and generation of formatted report to be submitted to the facility management organization. Table 1 is an example of limit states used for the condition evaluation of a cable stayed bridge. While the threshold of the limit states for those indices that can be obtained from the time domain responses can be determined directly from references and structural analyses, decision of limit states for changes in natural frequency of a major structural component such as pylon or cable needs chronical data for a reliable condition assessment.

Table 1. Response indices and limit states.

Response Indices	Values	Limits	Result	Limit States Decision
Peak ground acceleration	80 gal	110 gal	Safe	Design ground acceleration
Frequency change of the pylon	5%	16%	Safe	Empirical-chronical data
Frequency change of the cable	2%	10%	Safe	Empirical-chronical data
Max. vertical displacement of deck	230 mm	450 mm	Safe	Structural analysis
Max. torsion of deck	0.005 rad	0.01 rad	Safe	Structural analysis
Overall Condition Evaluation		Safe		

3. Measured Data and Condition Assessment

The analysis procedures and usability of the developed system are presented through the reference application for a cable-stayed concrete girder bridge (Figure 5). Locations of the seismic accelerometers are given in Figure 6. A three axes accelerometer is located at the base of one of the pylon. Two axes accelerometers are located at three locations; center of the deck, top of the pylon and deck height of the pylon. The bridge is located at the south coast of Korea peninsula. The height of the pylon and the length of the main span are 90 m and 230 m, respectively. A set of acceleration records were obtained from the reference bridge during an earthquake with magnitude of 5.0, which occurred off the coast of Ulsan, South Korea, on 5 July 2016. Locations of the bridge and the epicenter are shown in Figure 7. Since the reference bridge is 229 km away from the epicenter, the intensity of ground shaking was minor. The measured peak ground acceleration is 1.4 gal, which is only 0.93% of its design level earthquake intensity.

Figure 5. Overview of the reference bridge.

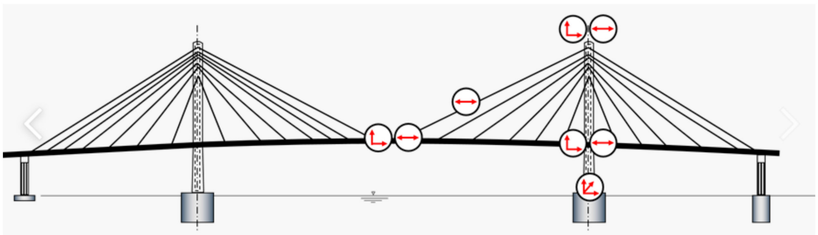

Figure 6. Location of the installed seismic accelerometers on the reference bridge.

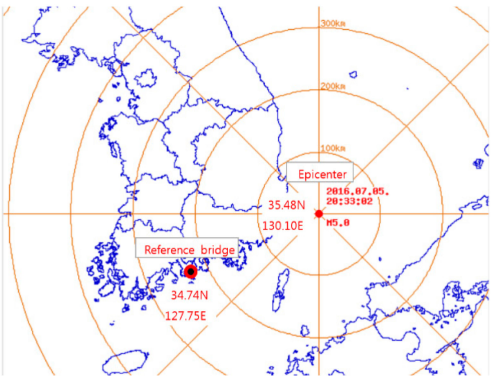

Figure 7. Location of the epicenter of the example earthquake.

As shown in Figure 2, all of the measured acceleration time histories are converted from the binary format of the miniSEED to the ASCII (American Standard Code for Information Interchange) format and this is followed by the synchronization process. Since some of the response indices in this system are based on the relative displacements synchronization of the acceleration time histories is necessary. After the format conversion and synchronization, noise filtering and base-line correction are carried out. The latter stage is followed by the calculation of the response indices for the condition assessment (Table 1). Details of the calculation procedure of the response indices are as follows:

(1) A peak ground acceleration was obtained by calculating the maximum absolute value of the horizontal acceleration time histories, which is the vector sum of the two horizontal components (North–South and East–West) of the accelerometer at the free field (Figure 8a). In this calculation, the vertical component was not accounted for. Figure 8b shows that the accelerations at the top of the pylon were much larger than those at the ground because the accelerations were amplified by the structural responses.

(2) A frequency change of the pylon was calculated by the percentage ratio of the change in the natural frequencies to the original of natural frequency. The natural frequency was obtained by identifying the location of the peak amplitude of the transfer function, which is the ratio of the Fourier amplitudes [37] of the top to the bottom. The results of the Fourier transformation performed on the measured data from the example earthquake are given in Figure 10. Details on the calculation of the transfer function are given elsewhere [38].

(3) A frequency change of the cable was calculated by the percentage ratio of the change in the natural frequencies to the original of natural frequency. The natural frequency was obtained by identifying the location of the peak of the Fourier amplitude, which is derived from the acceleration time histories at the center of the cable span in the vertical direction.

(4) A maximum vertical displacement of the deck is the peak value of the absolute of the vertical displacement time histories at the center of the deck (Figure 9b). Since there were two accelerometers at the center of the deck as shown in Figure 6, mean value of the vertical displacement of the two devices was used as the vertical displacement at the center of the deck. It is worth noting that the natural frequencies of the pylon and the deck could be implicitly estimated based on the observation on the distances between the peaks of the waves in the displacement time histories in Figure 9.

(5) A maximum torsion of the deck is the maximum value of the angle of torsion of the deck. The angle of torsion of the deck is calculated by the relative vertical displacement between the two accelerometers at the center of the deck divided by the width of the deck.

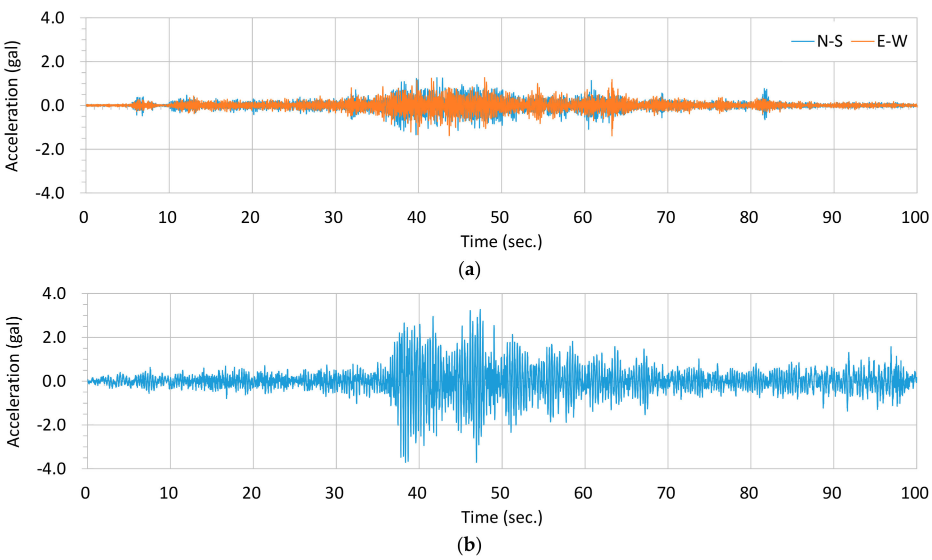

Figure 8. Measured time histories of the acceleration at the ground and top of the pylon. (**a**) Ground motion. (**b**) Top of the pylon.

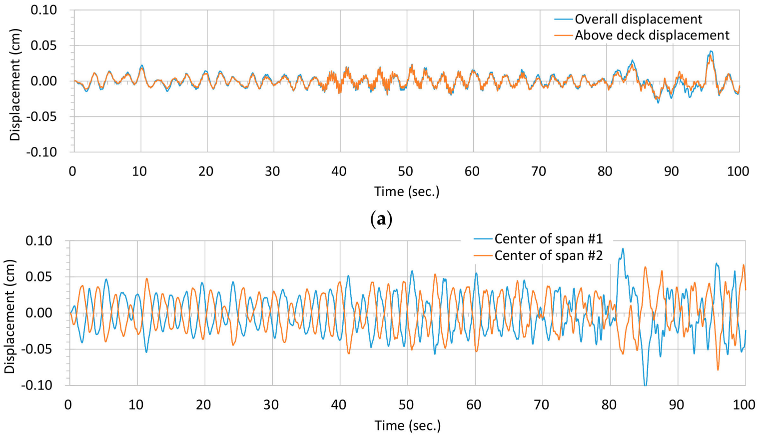

Figure 9. Displacement time histories. (**a**) Relative displacement of the pylon (longitudinal direction). (**b**) Vertical displacement of the center of the span.

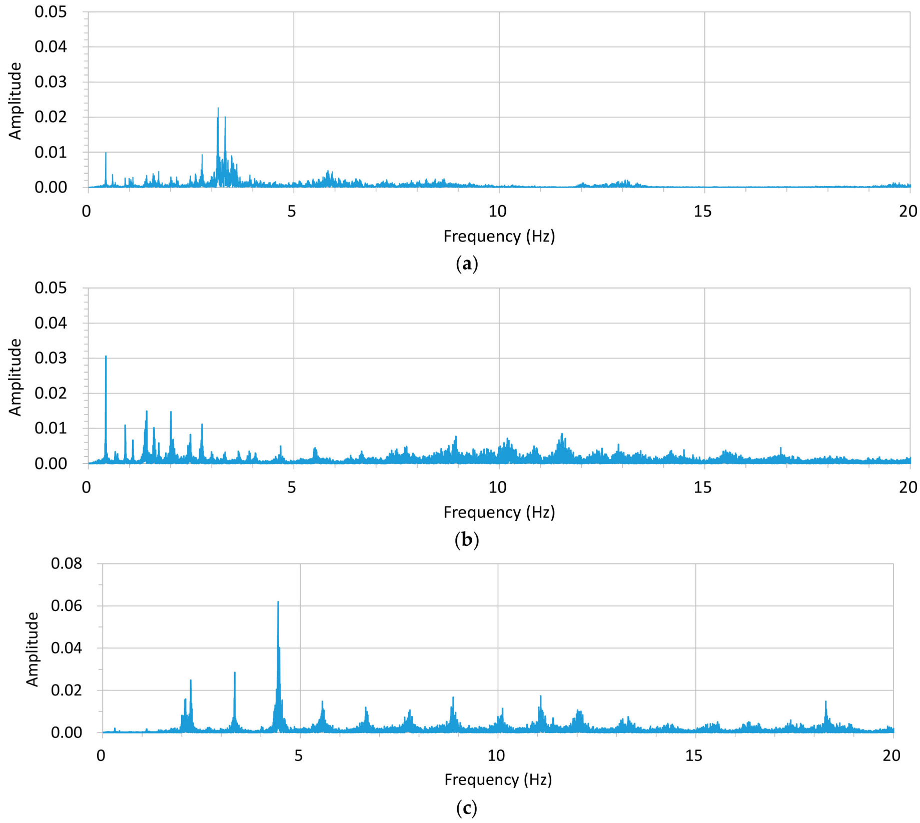

Figure 10. Fourier amplitude spectra of measured accelerations. (**a**) Top of the pylon (longitudinal direction). (**b**) Center of the span (vertical direction). (**c**) Cable (horizontal direction).

The result of the overall condition assessment should be derived based on the careful observation of the multiple response indices in Table 1. In general, for the safety reason, the worst case scenario is often assumed in the final decision, i.e., if one of the response indices were out of the safe boundary, the overall system would not be in the safe condition and need inspections. Despite the theoretical discussions given in this paper, unexpected errors in the field are the most difficult issue. Most of the latter problems may be dealt with by experienced field experts and these issues are beyond the boundary of this research. Determining a value of each of the limit states for the response indices requires is very difficult and requires huge amount of research effort. Since presenting the limit state is out of the boundary of this research, some examples of the limit states are given in Table 1.

4. Conclusions

A program for structural health monitoring of cable-stayed bridges using seismic accelerometers was developed. Various response indices in monitoring structural safety and serviceability of the bridges were discussed. Additional studies including a long term monitoring of field systems and statistical analyses were needed to better define the limit states of response indices for condition assessments. A systematic approach to process the raw data for generating appropriate response indices was proposed. The proposed system was composed of major components of a health monitoring software. The data matrix adopted in the system represents the interrelationship between the measured data from the seismic accelerometers and the response indices. A whole set of data in this system was organized in the form of 2D matrix. This form of data set was devised to pursue efficiencies in database accommodation and expandability to other structures. Through the reference application, it is shown that the proposed system of data process and the format of data organization could be used for the condition assessment of cable stayed bridges.

Author Contributions: Conceptualization, S.-H.J., J.-W.N. and H.A.; methodology, S.-H.J.; software, W.-S.J.; validation, D.-J.K.; formal analysis, J.-W.N. and H.A.; investigation, W.-S.J.; resources, J.-W.N. and H.A.; data curation, W.-S.J.; writing—original draft preparation, S.-H.J.; writing—review and editing, S.-H.J.; visualization, W.-S.J.; supervision, D.-J.K.; project administration, D.-J.K.; funding acquisition, J.-W.N. and H.A. All authors have read and agreed to the published version of the manuscript.

Funding: The research described in this paper was financially supported by Basic Science Research Program through the National Research Foundation of Korea (NRF) funded by the Ministry of Education (2017R1D1A1B03036358) and Inha University Research Grant.

Conflicts of Interest: The authors declare no conflict of interest.

References

1. Jang, S.; Jo, H.; Cho, S.; Mechitov, K.; Rice, J.A.; Sim, S.-H.; Jung, H.-J.; Yun, C.-B.; Spencer, B.F.; Agha, G. Structural health monitoring of a cable-stayed bridge using smart sensor technology: Deployment and evaluation. *Smart Struct. Syst.* **2010**, *6*, 439–459. [CrossRef]
2. Jo, B.-W.; Kim, H.; Lee, Y.-S.; Kim, D.-K. Development of real time smart structure monitoring system for bridge safety maintenance using sensor network. *J. Korea Concr. Assoc.* **2016**, *16*, 221–230. [CrossRef]
3. Choi, B.-G.; Sohn, D.-J.; Na, Y.-W. A study on the real time monitoring of long span bridge behavior using GPS. *J. Korean Soc. Surv. Geod. Photogramm. Cartogr.* **2010**, *28*, 377–383.
4. Chen, Y.; Xingwei, X. Advances in the structural health monitoring of bridges using piezoelectric transducers. *Sensors* **2018**, *18*, 4312. [CrossRef] [PubMed]
5. Cusson, D.; Lounis, Z.; Daigle, L. Durability monitoring for improved service life predictions of concrete bridge decks in corrosive environments. *Comput. Aided Civ. Infrastruct. Eng.* **2011**, *26*, 1–40. [CrossRef]
6. Ko, J.M.; Ni, Y.Q. Technology developments in structural health monitoring of large-scale bridges. *Eng. Struct.* **2005**, *27*, 1715–1725. [CrossRef]
7. Fujino, Y.; Siringoringo, D.M.; Ikeda, Y.; Nagayama, T.; Mizutani, T. Research and implementations of structural monitoring for bridges and buildings in Japan. *Engineering* **2019**, *5*, 1093–1119. [CrossRef]
8. Abe, M.; Fujino, Y. Bridge monitoring in Japan. In *Encyclopedia of Structural Health Monitoring*; Boller, C., Chang, F., Fujino, Y., Eds.; John Wiley & Sons Inc.: Hoboken, NJ, USA, 2009; pp. 2131–2148.
9. Siringoringo, D.M.; Fujino, Y. Observed dynamic performance of the Yokoha Bay Bridge from system identification using seismic records. *Struct. Control. Health Monit.* **2006**, *13*, 226–244. [CrossRef]
10. Luo, L.; Feng, M.Q.; Wu, Z.Y. Robust vision sensor for multi-point displacement monitoring of bridges in the field. *Eng. Struct.* **2018**, *163*, 255–266. [CrossRef]
11. Yu, S.; Zhang, J. Fast bridge deflection monitoring through an improved feature tracing algorithm. *Comput. Aided Civ. Infrastruct. Eng.* **2019**, *2019*, 1–11. [CrossRef]
12. Sekiya, H.; Kimura, K.; Miki, C. Technique for determining bridge displacement response using MEMS accelerometers. *Sensors* **2016**, *16*, 257. [CrossRef] [PubMed]
13. Ribeiro, R.R.; Lameiras, R.M. Evaluation of low-cost MEMS accelerometers for SHM: Frequency and damping identification of civil structures. *Lat. Am. J. Solids Struct.* **2019**, *16*, e203. [CrossRef]

14. Web, G.T.; Vardanega, P.J.; Middleton, C.R. Categories of SHM deployments: Technologies and capabilities. *J. Bridge Eng. ASCE* **2015**, *20*, 04014118. [CrossRef]
15. Pakzad, S.N.; Fenves, G.L. Statistical analysis of vibration modes of a suspension bridge using spatially dense wireless sensor network. *J. Struct. Eng.* **2009**, *135*, 863–872. [CrossRef]
16. Noel, A.B.; Abdaoui, A.; Elfouly, T.; Ahmed, M.H.; Badawy, A.; Shehata, M.S. Structural health monitoring using wireless sensor networks: A comprehensive survey. *IEEE Commun. Surv. Tutor.* **2017**, *19*, 1403–1423. [CrossRef]
17. Tokognon, C.A.; Gao, B.; Tian, G.Y.; Yan, Y. Structural health monitoring framework based on internet of things: A Survey. *IEEE Internet Things J.* **2017**, *4*, 619–635. [CrossRef]
18. Mahmud, M.A.; Bates, K.; Wood, T.; Abdelgawad, A.; Yelamarthi, K. A complete internet of things (IoT) platform for structural health monitoring (SHM). In Proceedings of the 2018 IEEE 4th World Forum on Internet of Things (WF-IoT), Singapore, 5–8 February 2018; pp. 275–279.
19. Kim, H.-S.; Kim, Y.-H.; Park, J.-C.; Shin, S.-B. Data analysis and health index for health monitoring of Seohae Bridge. *J. Korean Soc. Civ. Eng.* **2013**, *33*, 387–395. [CrossRef]
20. National Disaster Management Institute. *Development of the Public Buildings Emergency Integrity Assessment Technology using Seismic Acceleration Response Signal*; Research Report; National Disaster Management Institute: Ulsan, Korea, 2012.
21. National Disaster Management Institute. *Development of the Advanced Seismic Acceleration Analysis and Management System*; National Disaster Management Institute: Ulsan, Korea, 2013.
22. National Disaster Management Institute. *Development of Disaster Mitigation Technology Based on Vibration Measurement Data*; Research Report; National Disaster Management Institute: Ulsan, Korea, 2014.
23. IRIS. *SEED Reference Manual*; SEED Format Version 2.4; IRIS: Washington, DC, USA, 2012.
24. Mollova, G. Effects of digital filtering in data processing of seismic acceleration records. *EURASIP J. Adv. Signal Process.* **2007**, *2007*, 29502. [CrossRef]
25. Cherry, S. Earthquake ground motion: Measurement and charicteristics. In *Engineering Seismology and Earthquake Engineering*; Solnes, J., Ed.; NATO Advanced Study Institute Series; NATO Advanced Study Institute: Brussels, Belgium, 1974; pp. 87–124.
26. Kanai, K.; Tanaka, T. On Microtremors. VIII. *Bull. Earthq. Res. Inst.* **1961**, *39*, 97–114.
27. Korea Institute of Geoscience & Mineral Resources. *Construction and Operation of Earthquake Research Stations*; Research Report; Korea Institute of Geoscience & Mineral Resources: Daejeon, Korea, 2000.
28. Boore, D.M.; Bommer, J.J. Processing of strong-motion accelerograms: Need, options and consequences. *Soil Dyn. Earthq. Eng.* **2005**, *25*, 93–115. [CrossRef]
29. Ministry of Land. *Infrastructure and Transport, Structural Health Monitoring Based on Displacement*; Research Report; Ministry of Land: Sejong City, Korea, 2014.
30. Salawu, O.S. Detection of structural damage through changes in frequency: A review. *Eng. Struct.* **1997**, *19*, 718–723. [CrossRef]
31. Vandiver, J.K. Detection of structural failure on fixed platforms by measurement of dynamic response. *J. Pet. Technol.* **1977**, *29*, 305–310. [CrossRef]
32. Idichandy, V.G.; Ganapathy, C. Modal parameters for structural integrity monitoring of fixed offshore platforms. *Exp. Mech.* **1990**, *30*, 382–391. [CrossRef]
33. Zhou, Y.L. Structural Health Monitoring by Using Transmissibility. Ph.D. Thesis, Universidad Politécnica de Madrid, Madrid, Spain, 2015.
34. Wahab, M.M.A.; Roeck, G.D. Damage detection in bridges using modal curvatures: Application to a real damage scenario. *J. Sound Vib.* **1999**, *226*, 217–235. [CrossRef]
35. Zhao, L.; Huang, X.; Zhang, Y.; Tian, Y.; Zhao, Y. A vibration-based structural health monitoring system for transmission line towers. *Electronics* **2019**, *8*, 515. [CrossRef]
36. He, K.; Zhu, W.D. Structural damage detection using changes in natural frequencies: Theory and applications. *J. Phys. Conf. Ser.* **2011**, *305*, 1–10. [CrossRef]

37. Brigham, E.O. *The Fast Fourier Transform and Its Application*; Prentice Hall: Englewood Cliffs, NJ, USA, 1998.
38. Ljung, L. *System Identification: Theory for the User*; Prentice Hall: Englewood Cliffs, NJ, USA, 1987.